DYNAMICS OF THE AIR BLOWER WITH GYROSCOPIC COUPLE

Marius Vasylius[*], Vytautas K. Augustaitis[**], Vytautas Barzdaitis[***], Marijonas Bogdevicius[****]

[*]Klaipeda University, Mechatronics Science Institute, Bijunu str. 17, LT-91225 Klaipeda, Lithuania
[**]Vilnius Gediminas Technical University, Department of Machine Building, J. Basanaviciaus str. 28, LT-32214,Vilnius, Lithuania
[***]Kaunas University of Technology, Engineering Mechanics Department, A. Mickeviciaus str. 37, LT-44244, Kaunas, Lithuania
[****]Vilnius Gediminas Technical University, Department of Transport Technological Equipment,
Plytines St. 27 LT-10105, Vilnius, Lithuania

mvasylius@yahoo.com, pgkatedra@me.vtu.lt, vytautas.barzdaitis@ktu.lt, marius@ti.vgtu.lt

Abstract: To avoid damaging of tilting pad journal bearings, the problem of safety shut down of high speed air blower cantilever rotor becoming important in modern industry. The experimental testing, modeling and simulation of dynamic behavior of rotating system was run to directly evaluate gyroscopic negative effect damaging journal bearings. A dynamic model of air blower rotating system was designed and simulated. A simulation and experimental measurement results of rotating system were used to optimize the shut down regime of machine. Gyroscopic effect influences of rotor bearing stability are confirmed. Results of numerical simulation confirm results of experimental vibration measuring. The theoretical research results are given and conclusions are made. Experimental testing and simulations results was applied to typical air blower rotating systems for elimination of huge negative forces acting on new bearings during shut down of the machine.

1. INTRODUCTION

One of most often problems occurring rotating system exploitations is high vibration displacements of journal in tilting pad bearings. The general causes of these vibrations are unbalance, insufficient dynamic stiffness, mechanical looseness and rotating elements wear, etc. (Bently, 2002)

Rotors of turbines, compressors, fans and etc. carry one or more disks, and these disks besides contributing to a lumped mass at stations where they are located, also introduce a gyroscopic couple. The effect of gyroscopic couple is predominant, if the disk is located at a nodal point or at a free end of the rotor (Rao, 1996) . The effect of gyroscopic couple has been researched in many papers, starting from pioneering works by Smith (1933), Yamamoto (1954), Dimentberg (1961), considering various ways of unfolding the rotor lateral transversal and angular motion. Descriptions of gyroscopic effects, together with more complete lists of references, can be found in publications by Ehrich (1992) and by Vance (1988). An experimental work dealing with parameter identification for the rotor system with large gyroscopic influence was reported by D. Bently et al. (1986) (Muszynska, 2005).

Technological critical machinery is expensive. They cannot be replaced. The stoppage or breakdown of these machines are destructive to all technological process and associated with big economical losses. That is the main reason to estimate the technical condition of the machinery by using technical condition monitoring, protection and failure diagnostics and particular unexpected breakdown preventions systems (Barzdaitis and Činikas, 1998).

The purpose of this paper is to design the mathematical model of air blower rotor's system, which describes the vibrations of the system and to identify the sources of the vibrations: dynamic stiffness of bearing support, the rotor's systems resonance frequency and identify the influence of gyroscopic effect of rotor vibration.

2. ROTATING SYSTEM OF AIR BLOWER MACHINE

The air blower machine SF01-18 comprises high power electric motor EM, gear box GB and blower rotor BR, as shown in Fig. 1. The induction motor (power 5.6 MW) runs at 1500 rpm and rotates an air blower rotor BR through flexible 8 pin type coupling C1, gear box GB and flexible type coupling C2 at high rotational speed at 3119 r/min.

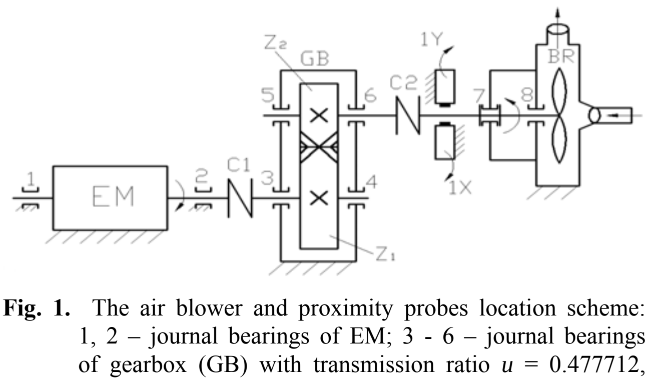

Fig. 1. The air blower and proximity probes location scheme: 1, 2 – journal bearings of EM; 3 - 6 – journal bearings of gearbox (GB) with transmission ratio u = 0.477712, z_2 = 43 of a driven gear and z_1 = 90 of a driving gear; 7, 8 – tilting-pad journal bearings of blower rotor (BR); C1, C2 – flexible couplings; 1X, 1Y – proximity probes fixed at the 7[th] bearings

For technical condition monitoring and vibration data analyzing has been used diagnostic equipment Dynamic Machine Analyser DMA04 (Epro, Germany, Profess s.r.o., Czech Republic), with software MMS 6850 Database (Adash s.r.o. Czech Republic). The technical condition is evaluated by monitoring of air blower rotor vibration displacement permanently.

In this article we studied dynamics behavior of blower rotor pivoted-pad journal bearings. The objective is to determine the main reason of the journal bearings failure. The blower rotor shaft vibration displacement $s_{p\text{-}p7}$ and s_{max7} values at 7th bearing and maximum vibration displacement s_{max} values of the shaft at the middle location point between 7th and 8th bearings monitored by means of 7X, 7Y proximity probes, contact less measurement induction sensors.

3. RESULTS OF EXPERIMENTAL INVESTIGATION

The experimental testing of the blower rotor vibration made at different running modes: at nominal loading 100 % and 50 % and at free run. The blower rotor resonance speeds measured at run up and coast down regimes. The 7th bearing shaft vibration displacements and orbits at full loading and coast down running mode are presented in Fig. 2a and Fig 2b.

The peak-to-peak vibration displacement values at resonance speed 1436 rpm reached inaccessible values in both *X* and *Y* orthogonal directions as shown in vibration displacements plots and orbit of the shaft, Fig. 2b. These vibration displacements $\boldsymbol{s_{p\text{-}p}}$ values became 6-8 times higher at the resonance in comparison with values at the maximum load at 3119-3132 rpm (Fig. 2a). The blower rotor high vibration displacements at resonance mode damage the journal bearings. The valuable damages are checked at the upper segment of the 7th bearing and the lower segment of the 8th bearing.

The dynamic forces that damages bearings depend not only by resonance phenomenon but by rotors gyroscopic effect too. The rotors shaft position in the 7th bearings is described by the gap value. When machine runs in coast down mode, the gap between the vertical sensor 7*Y* tip and shaft surface decreases about ~200 µm value reference to nominal position at maximum rotation speed.

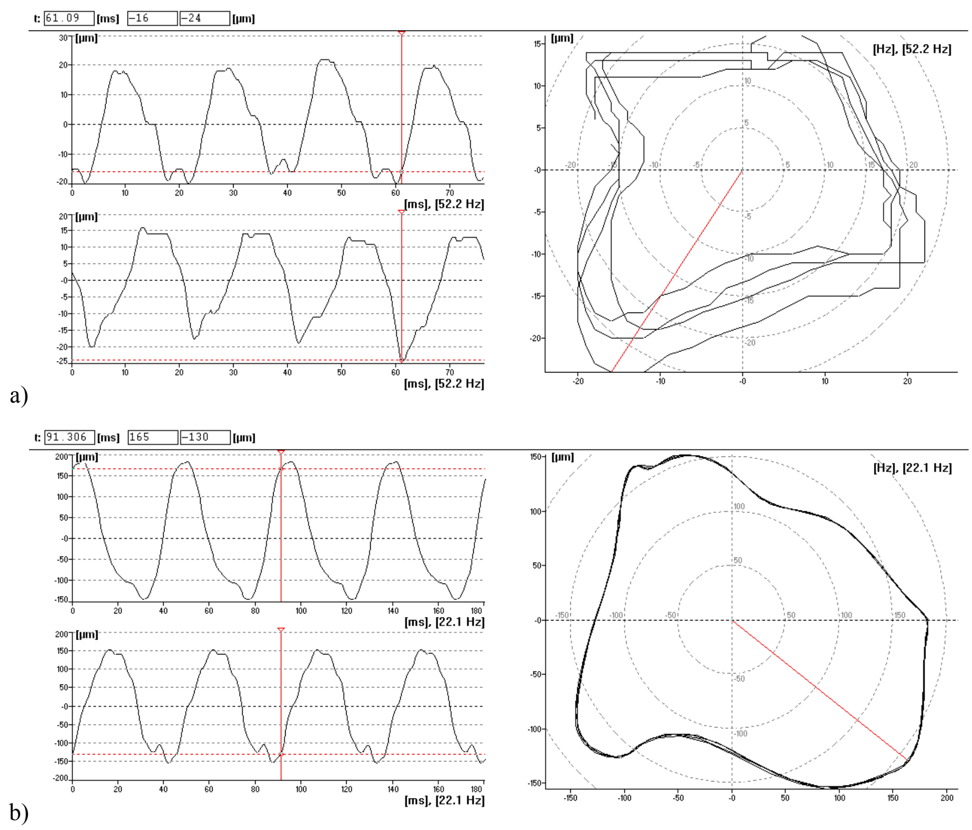

Fig. 2. The vibration displacements plots and orbits of blower rotor measured at bearing 7th at full loading (a): $\boldsymbol{s_{(o\text{-}p)x}}$ = ~22µm, $\boldsymbol{s_{(o\text{-}p)y}}$ = ~20µm and $\boldsymbol{s_{max}}$ = 27µm at 3132 rpm and at coast down, (b): $\boldsymbol{s_{(o\text{-}p)x}}$ = 183µm, $\boldsymbol{s_{(o\text{-}p)y}}$ =155µm and $\boldsymbol{s_{max}}$ = 210µm at 1324rpm

4. MODELING AND SIMULATION OF BLOWER ROTOR

The purpose of the mathematical modeling is to confirm a gyroscopic effect hypothesis and to estimate the influence of dynamics forces to bearings durability. The rotor dynamics is analyzed by the finite-element method, where the finite element consists of two nodes and five degrees (DOF) at each node. The first and the second DOF are displacements along the *y* and *z* axes and the last three DOF are angles around *X*, *Y* and *Z* axes.

The dynamic model of all system in static state is shown in Fig. 3.

There are three coordinate systems of axes to localize rotor position (Fig. 4):

1) Inertia coordinate system *OXYZ*. Point *O* in steady state coinsides with the point where rotor is attached to the blower.
2) In the moving coordinate system $O_1Y_1Z_1$ point O_1 is tightly connected to the rotor. When rotor rotates, geometrical center O_1 moves in plane *OYZ*.
3) Coordinate system $O_CY_CZ_C$ of mass center. Any rotor point P position is defined by vector $\vec{r}_{cp}$.

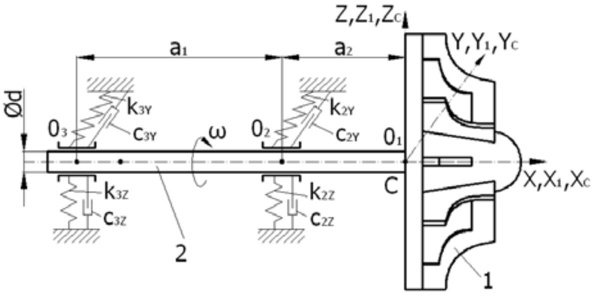

Fig. 3. Dynamic model of the air blower rotor: 1 – air blower, 2 – rotor, d = 0.20m, a_1 = 0.844 m, a_2 = 0.5m

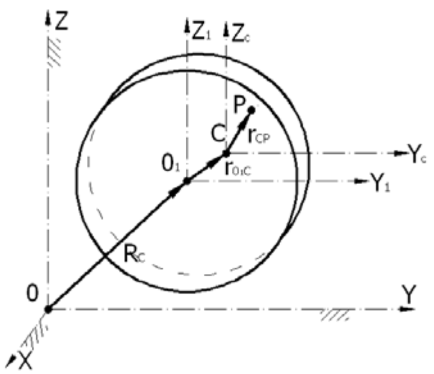

Fig. 4. The scheme of coordinates and vectors deployment which describe the rotor position

Work variation of inertial forces:

$$\delta W = \int_m \left\{\delta R_p\right\}^T \left\{\ddot{R}_p\right\} dm ; \qquad (1)$$

Where $\{\delta R_p\}^T$ – variation vector of point P; $\left\{\ddot{R}_p\right\}$ – acceleration vector of point P.

The system of equations of blower:

$$\left[I_b\right]\left\{\ddot{\theta}\right\} = \left\{F_b\left(\theta,\dot{\theta},t\right)\right\} ; \qquad (2)$$

where

$$I_b = \begin{bmatrix} I_{x1x1} & -I_{x1y1} & -I_{x1z1} \\ -I_{y1x1} & I_{y1y1} & -I_{y1z1} \\ -I_{z1x1} & -I_{z1y1} & I_{z1z1} \end{bmatrix} \quad - \quad \text{mass interia tensor of blower}$$

$\left\{F_b\left(\theta,\dot{\theta},t\right)\right\}$ – vector of forces which affecting blower.

Mass inertia tensor of blower:

$$\left[I_b\right] = \left[I_c\right] + \left[M_b\right]\left[\tilde{r}_{01c}\right]^T\left[r_{01c}\right] + \left[\tilde{r}_{01c}\right]^T\left[\tilde{S}\right] + \left[\tilde{S}\right]^T\left[\tilde{r}_{01c}\right] ; \qquad (3)$$

where $\left[I_c\right]$ – mass inertia tensor in respect of mass center. $I_c = \int_V \rho\left[\tilde{r}_{cp}\right]^T\left[\tilde{r}_{cp}\right] dV$; $\left[M_b\right]$ – mass matrix of blower; $\left[M_b\right] = diag\left(m_b, m_b, m_b\right)$; $\left[\tilde{r}_{01c}\right]$ – skew-symmetric matrix associated with vector $\left\{r_{01c}\right\}$; $\left[\tilde{S}\right]$ – skew-symmetric matrix associated with vector $\left\{S\right\} = \int \rho\left(\left\{r_{01c}\right\} + \left\{r_{cp}\right\}\right) dV$; $\left\{r_{cp}\right\}$ – vector defined position of either blower point in respect of mass center C.

Vector of forces and moments which affecting blower:

$$\left\{F_b\right\}^T = \left[\left\{F_{bR}\right\}^T, \left\{F_{b\theta}\right\}\right] ; \qquad (4)$$

where $\{F_{bR}\}$– vector of forces which affecting blower. It calculable:

$$\left\{F_{bR}\right\} = -\left[\tilde{\omega}\right]\left[A\right]\left\{S\right\} + \left[A\right]\left[\tilde{S}\right]\left[A\right]^T\left[\dot{G}_2\right]\left\{\dot{\theta}\right\} ; \qquad (5)$$

where $\left[\tilde{\omega}\right]$ – Matrix of angular velocity; [*A*] – transformation matrix between global and local coordinate systems; $\left[\dot{G}_2\right]$ – derivate of matrix $\left[G_2\right]$ by time in global coordinate system; $\left\{\dot{\theta}\right\}$ – vector of derivate of turning angle. $\left\{F_{b\theta}\right\}$ – vector of moments which affecting disk. It calculable:

$$\left\{F_{b\theta}\right\} = -\left[\underline{G}_2\right]^T\left[\tilde{\underline{\omega}}\right]\left[I_b\right]\left\{\underline{\omega}\right\} + \left[\underline{G}_2\right]^T\left[I_b\right]\left[A\right]^T\left[\dot{G}_2\right]\left\{\dot{\theta}\right\} ; \qquad (6)$$

where $\left[\tilde{\omega}\right]$ – skew-symmetric matrix associated with vector of angular velocity in body coordinate system. $\left\{\underline{\omega}\right\}$, $\left[\tilde{\underline{\omega}}\right] = \left[A\right]^T\left[\tilde{\omega}\right]\left[A\right]$; $\left[\tilde{\underline{\omega}}\right]$ – skew-symmetric matrix associated with vector of angular velocity in the inertia coordinate system.

Transformations of coordinate:

$$\left\{R_{01}\right\} = \left[B_1\right]\left\{q\right\} ;$$

where $[B_1]$ – transformations of coordinate.

Angles, first and second derivates of angles vector velocities and accelerations:

$$\left\{\theta\right\} = \left[N_\theta\right]\left\{q\right\}; \quad \left\{\dot{\theta}\right\} = \left[N_\theta\right]\left\{\dot{q}\right\}; \quad \left\{\ddot{\theta}\right\} = \left[N_\theta\right]\left\{\ddot{q}\right\}. \qquad (7)$$

where $[N_\theta]$ – matrix of element form function.

Vector of blower generalized coordinates:

$$\left\{q_b\right\} = \left[B\right]\left\{q\right\} ; \qquad (8)$$

The system of equation of blower motion:

$$\left[B\right]^T\left[M_b\right]\left[B\right]\left\{\ddot{q}\right\} = \left[B\right]^T\left\{F_b\left(q,\dot{q},t\right)\right\} ; \qquad (9)$$

The equations of motion of rotor's finite element are derived by applying a Lagrange equation of the second order, which can be written as follows:

$$\left(\left[M_e\right]+\left[B\right]^T\left[M_b\right]\left[B\right]\right)\left\{\ddot{q}\right\}+\left(\left[C_e\right]+\left[G_e\right]\right)\left\{\dot{q}\right\}+ \left[K_e\right]\left\{q\right\}=\left\{F_e\left(q,\dot{q},t\right)\right\}+\left[B\right]^T\left\{F_b\left(q,\dot{q},t\right)\right\}; \quad (10)$$

where $[M_e]$, $[M_b]$, $[C_e]$, $[G_e]$, and $[K_e]$ are mass of finite element, mass of blower, damping, gyroscopic and stiffness matrices of the finite element, respectively;

$\left\{F_e\left(q,\dot{q},t\right)\right\}$ and $\left\{\vec{F}_b\left(q,\dot{q},t\right)\right\}$ are vectors of forces which affecting rotors finite element and blower.

General equation of all rotating system in matrix form:

$$\left[M\right]\left\{\ddot{q}\right\}+\left[C\right]\left\{\dot{q}\right\}+\left[K\right]\left\{q\right\}=\left\{F\left(q,\dot{q},t\right)\right\} \quad (11)$$

where $[M]$, $[C]$, $[K]$ are the mass, damping and stiffness matrices; $\left\{F\left(q,\dot{q},t\right)\right\}$ is a non-linear force vector; $\{q\}$, $\{\dot{q}\}$ and $\{\ddot{q}\}$ are the displacement, velocity and acceleration vectors of the finite-element assemblage. In an implicit time-integration scheme, the equilibrium of the system (11) is considered at time $t + \Delta t$ to obtain the solution at time $t + \Delta t$. Iteration will be performed in the non-linear analysis (Barzdaitis and Bogdevičius, 2006).

5. RESULTS OF THEORETICAL INVESTIGATION

The calculation results are shown in Fig. 5 and Fig. 6. There is orbit plot of the rotor center O_2, were rotor is attached to air blower, Fig. 5. Numerical calculation results approved that vibration displacement of the rotor are caused not only by unbalance, but by gyroscopic effect too.

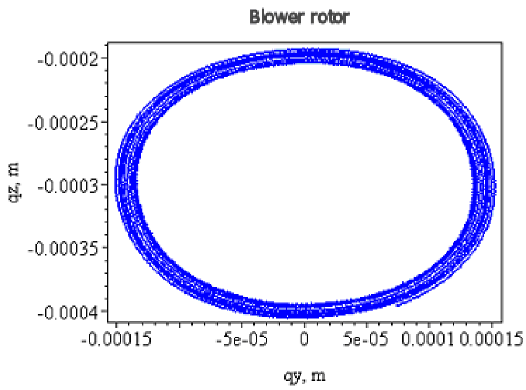

Fig. 5. Orbit of the rotor center point O_2 at nominal rotation speed 3120 rpm, $s_{p\text{-}pmax}$ = 300 μm.

In Fig. 6 are shown orbit of the shafts rotating in 7^{th} and 8^{th} bearings. The four pad tilting-pad journal bearing model of the rotating system was used. The numerical calculation results were acquired with such parameters: coefficients of stiffness of bearing $k_{3Y}=k_{3Z}=200\times10^6$N/m, $k_{2Y}=k_{2Z}=150\times10^6$N/m; coefficients of damping $c_{3Y}=c_{3Z}=40\times10^3$Ns/m, $c_{2Y}=c_{2Z}=20\times10^3$Ns/m; rotor diameter d=0.20m; air blower weight m=1660kg.

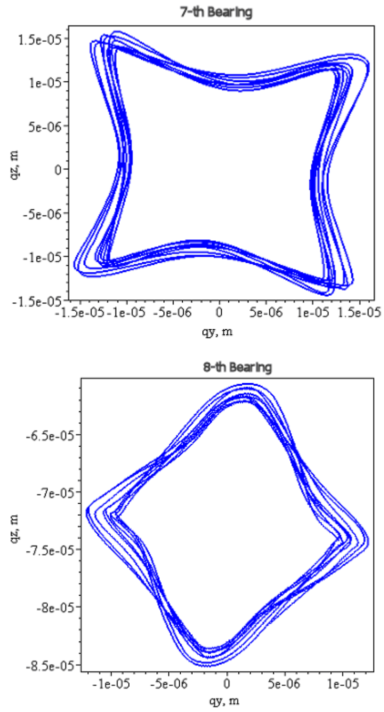

Fig. 6. Simulation results of the journals motion in the bearings at nominal rotating speed 3120rpm. a) – orbit of 7th bearing $s_{p\text{-}pmax}$=31μm, b) – orbit of 8th bearing $s_{p\text{-}pmax}$=25μm

6. CONCLUSIONS

1. The designed theoretical model of the air blower rotating system is based on the finite-element method.
2. Calculation and experimental results indicated that gyroscopic effect is important for long continuous run of
   tilting pad journal bearings. Elevated hypothesis is that air blower rotors gyroscopic moment decrease rotor dynamic eccentricity at nominal rotating speed.
3. But during shutdown mode of operation its negative influence of the tilting pad bearing wear is inadmissible too high.
4. Air blower rotating system shutdown time interval must be minimized with additional brake mechanism.

REFERENCES

1. **Barzdaitis V., Bogdevičius M.** (2006), The Dynamic Behavior of a Turbine Rotating System/ Strojniski vestnik, *Journal of Mechanical Engineering*, 5210, 653-661.
2. **Barzdaitis, V., Činikas G. (1998)**, *Monitoring and Diagnostics of Rotor Machines*, Kaunas: Technologija, Lithuania.
3. **Bently D. E.** (2002), *Fundamentals of Rotating Machinery Diagnostics*, Library of Congress Control, Bently Pressurized Bearing Company.
4. **Muszynska A.** (2005), *Rotordynamics*, CRC.
5. **Rao J. S.** (1996), Rotor Dynamics 3th edition, New Age Publishers.